The International Journal of Advanced Manufacturing Technology (2018) 97:953–965
https://doi.org/10.1007/s00170-018-1945-6

ORIGINAL ARTICLE

Roll formability of aluminium foam sandwich panels

Matthias Weiss[1] · Buddhika Abeyrathna[1] · Michael Pereira[2]

Received: 13 November 2017 / Accepted: 20 March 2018 / Published online: 16 April 2018

Abstract
An aluminium foam sandwich (AFS) material was formed by V-die bending and roll forming. The V-bent sections showed material failure by shear fracture of the aluminium foam core and by delamination at the core-cover sheet interface. This led to a high-gull wing defect and a limited section depth that could be formed. In contrast, the roll forming process allowed the manufacture of long sections with acceptable profile depth. Only minor gull wing was observed, and this was related to a low-shear deformation of the aluminium foam core and an intact adhesion at the core-cover sheet interface. The higher material formability observed in roll forming compared to that in V-die bending was attributed to a more evenly distributed contact pressure and more homogeneous forming, due to the incremental nature of the process, combined with a continuous contact of the metal sheet with the top and bottom rolls. Some forming problems were also observed in the roll-formed AFS components, but overall, the results of this study suggest that roll forming represents a good alternative to bending or stamping for the forming of longitudinal components of simple cross section shape that are of interest to the transport, solar or housing industries.

Keywords Aluminium foam · Sandwich · Bending · Roll forming · Gull wing defect

1 Introduction

Aluminium foam sandwich (AFS) panels are new light-weight products. They consist of a porous aluminium interlayer that is bonded to two aluminium cover sheets [1]. This gives AFS panels a high stiffness to weight ratio combined with good thermal insulation properties and excellent sound and vibration-damping capabilities [2]. AFS materials are promising light-weight solutions for the aerospace and the automotive sector, but this requires the AFS materials to be formed into complex shapes. One strategy involves the forming of foamable precursors that contain a blowing agent and are bonded to two metal face sheets [1, 3]. After forming, the core is expanded by heating to the foaming temperature of the blowing agent. The advantage of this method is that the core material is formed in a compact condition which makes it less likely to be crushed by the forming tools or to fracture when sheared. Nevertheless, the process limits the alloys that can be used and is restricted to closed pore foams [4]. Only a few studies have focused on the direct forming of AFS panels. In the channel drawing of AFS material, Contorno et al. [5] observed extensive core shear deformation which led to early failure by core extrusion and delamination at the core-cover sheet interface. In addition, extensive thinning of the laminate was observed due to the crushing of the foam core layer. A similar observation was made by Jackson et al. [6] for the incremental forming of AFS components, where compressive deformation of the foam core led to an uneven part surface and delamination. Also in gas pressure forming, compression of the foam core was observed and this led to thickness reductions of the overall AFS laminate of up to 40% [4]. In hydroforming, crushing of the core layer could be avoided by filling the porous foam core with pressure fluid; however, component complexity still remained limited due to delamination at the core-cover sheet interface [7].

When bend-forming metal laminates that have two cover sheets of high strength with a softer interlayer, it is well known that shear deformation of the core material occurs [8]. For AFS sheets with low-adhesion strength at the core-cover sheet interface, this can lead to component failure by delamination [9]; while in cases where adhesion is high, shear failure by cracking

✉ Matthias Weiss
mweiss@deakin.edu.au

[1] Institute for Frontier Materials, Deakin University, Waurn Ponds, Pigdons Rd, Geelong, VIC 3216, Australia

[2] School of Engineering, Deakin University, Waurn Ponds, Pigdons Rd, Geelong, VIC 3216, Australia

of the foam core has been observed [9]. Mohr [10] suggested that for the successful forming of AFS materials, adhesion and shear strength of the core needs to be as high as possible. Strengthening of the foam core can be achieved by reducing the pore size, but this increases core density and reduces the light-weight potential of the laminate. On the other hand, the thickness of the core can be decreased to lower the shear deformation during forming but this reduces the load-bearing capability of the laminate [11]. Improvements in the forming properties of laminates are therefore limited, and this suggests that alternative forming methods that lead to lower compression and lower shear deformation of the foam core are required.

In conventional sheet forming, the initially flat metal sheet is generally forced by an upper tool into a die cavity. This leads to localised contact on the tool profile radii and, in the case of AFS sheets, has been shown to result in localised indentation of the metal cover sheet and high-shear deformation in the core layer [12]. The roll forming process promises lower and more evenly distributed tool contact compared to conventional sheet forming. In roll forming, the sheet is incrementally bent into shape by passing it through successive roll stands [13] and the process allows forming of materials that combine high strength with limited ductility [14]. For this reason, roll forming is increasingly used in the automotive industry for the forming of long crash and structural components [15]. In roll forming, the material is usually supported by an upper and a lower tool and this has been shown to reduce localised or unstable deformation that is often observed when conventionally bending hard-to-form materials [16]. The more evenly distributed tool contact in roll forming promises to lower compression and shear deformation of the foam core layer, and this may lead to increased forming limits when shaping AFS materials. Therefore, roll forming may allow the cost-effective production of long components of simple cross sectional shapes from AFS sheets for potential applications in the transport, building or solar panel industries [2].

The scope of this study is to experimentally investigate the possibility of roll forming simple section shapes from a commercially available AFS panel as an alternative to the commonly used V-die bending process. To understand forming defects, such as material thinning due to the compression of the foam layer or laminate failure by delamination at the core-cover sheet interface, the mechanical properties of the laminate are investigated in the initial part of this work. The individual mechanical properties of the cover sheets and the foam core are determined by conventional tensile and adhesion tests on the metal cover sheets and the laminate, respectively. To understand the adhesion strength at the core-cover sheet interface, double lab shear tests are performed, while the tendency for compressive deformation of the foam core is analysed by compression tests. Comparison with previous studies is performed to verify the results. In the second part of the work, the forming of the same V-shaped profile is experimentally investigated for roll forming and V-die bending. The final part shape and forming defects, as well as the level of compression and shear deformation of the foam core, are compared between both processes. The results show that shear deformation in the foam core is lower in roll forming compared with that in the V-die bending process and that this allows the forming of tighter profile radii using roll forming. Nevertheless, due to the bending and re-straightening of the strip when entering the roll station, delamination at the core-cover sheet interface is observed for roll-formed parts. This is related to a low-adhesion strength and is common for ex-situ bonded AFS materials, where the cover sheets and the core layer are bonded with an adhesive layer after the interlayer material has been foamed. The problem may be overcome by roll forming AFS materials that have a metallic bond with inherently higher adhesion strength at the core-cover sheet interface. Overall, the results of this study suggest that roll forming may be a promising alternative to conventional bending or stamping for the manufacture of long and simple components from AFS sheets.

2 Experimental setup

2.1 Material

The material analysed in this study is an industrially produced ex-situ bonded AFS panel. The materials consist of two 1 mm cover sheets of AW 5754 aluminium that are bonded to a 6.2 mm thick ALPORAS® aluminium foam core using a 2-Komponenten-polyurethane (PUR)-adhesive, as shown in Fig. 1.

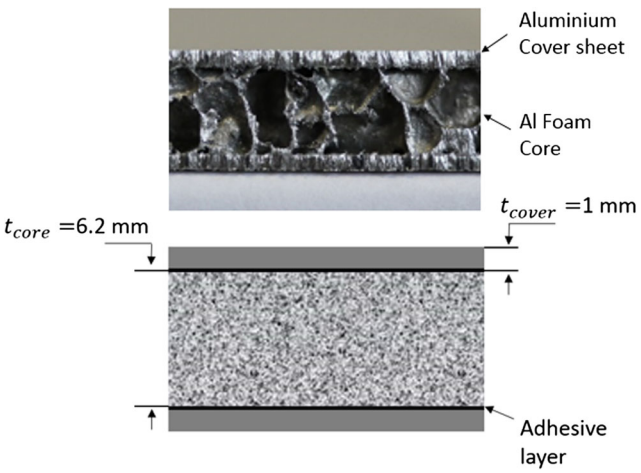

Fig. 1 Picture and schematic side view of the AFS panel

2.2 Uniaxial tensile tests

Tensile tests were performed at room temperature on the cover sheet material using a 50 kN Instron hydraulic test frame according to Australian Standard AS 1391–1991 [17]. Specimens oriented at 0° and 90° to the rolling direction were cut. To separate the cover sheets from the core material, first a cut was performed through the core layer and parallel to the cover sheet using a band saw. After this, a milling machine was used to remove the remaining core layer material from the cover sheets. The sample gauge length was 50 mm, a video extensometer was used to measure the engineering strain and a cross-head speed of 2 mm/min was used. At least four tests were performed and averaged for each specimen orientation. The Swift (Eq. 1) hardening equation was fitted to the true stress–strain ($\sigma - \varepsilon$) data for each sample direction tested.

$$\sigma_y = K\left(\varepsilon_0 + \varepsilon_p\right)^n \tag{1}$$

In the above equation, K is the strength coefficient, n is the strain-hardening exponent, ε_0 the strain offset constant and ε_p the equivalent plastic strain.

2.3 Lap shear test

To analyse the shear strength of the interlayer, double lap shear tests [18] were performed using the test sample arrangement shown in Fig. 2. The tests were performed using a 50 kN Instron hydraulic test frame. The specimens were fixed in the tensile grips of the machine, and a standard upper cross-head displacement of 0.5 mm/min was used as previously suggested in [19]. During the test, the shear reaction force, F_S,on the upper cross head was recorded while the displacement, Δl,relative to the two marks positioned on the sample was determined with a video extensometer.

The shear strain and stress, γ and τ, respectively, were determined using the relations

$$\gamma = \frac{\Delta l}{t_{\text{core}}} \tag{2}$$

and

$$\tau = 0.5\frac{F_s}{wl_s} \tag{3}$$

with the core thickness, t_{core}, the sample width, w, and the shear test length, l_s.

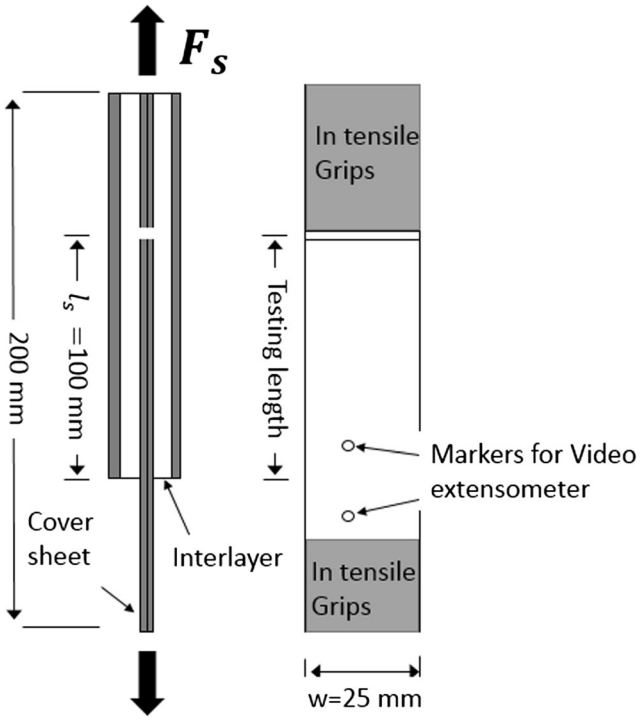

Fig. 2 Schematic of the lap shear test sample and arrangement

2.4 Adhesion test

The tensile adhesion strength between the core and the cover sheet was determined using the procedure described in [20] and the fixture and test setup shown in Fig. 3. Square-shaped specimens of side length $L = 50$ mm were cut using a band saw and glued to the testing blocks using "Araldite Super Strength", a two-part epoxy paste adhesive. The tests were performed in the 50 kN Instron hydraulic test frame. The reaction force, F_a, was measured on the upper cross head while the relative displacement of two markers, Δl, positioned on both cover sheets was determined with a video extensometer.

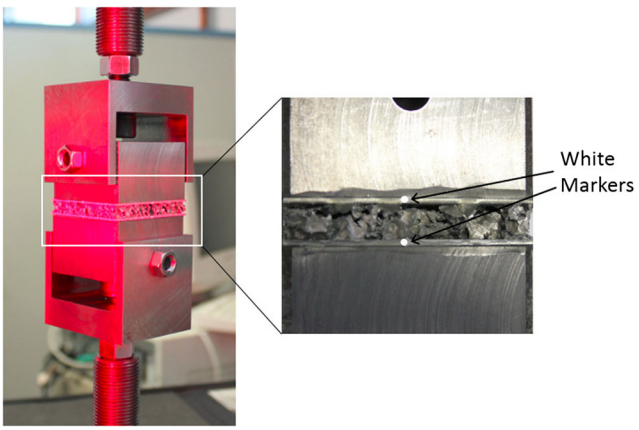

Fig. 3 Adhesion test. Sample between test plates showing the white markers applied for strain analysis

The adhesion strain and stress, ε_a and σ_a, respectively, were analysed using the relations

$$\varepsilon_a = \frac{\Delta l}{t_{\text{core}}} \tag{4}$$

and

$$\sigma_a = \frac{F_a}{L^2} \tag{5}$$

2.5 Compression test

For the compression tests, square-shaped samples of side length $L = 50$ mm were placed between two loading platens that were attached to a 50-kN Instron hydraulic test frame and a negative cross-head displacement of 0.5 mm/min applied (Fig. 4).

During the test, the compression force, F_c, was measured. Similar to the adhesion test setup, the relative displacement of the two markers, Δl, positioned on both cover sheets was determined with a video extensimeter. The maximum cross-head displacement was limited to half the core thickness, given that after this value the aluminium form core mainly deformed by compaction with an abrupt increase in the compression reaction force. Compressive stress and strain, ε_c and σ_c, respectively, were analysed using the relations

$$\varepsilon_c = \frac{\Delta l}{t_{\text{core}}} \tag{6}$$

and

$$\sigma_c = \frac{F_c}{L^2} \tag{7}$$

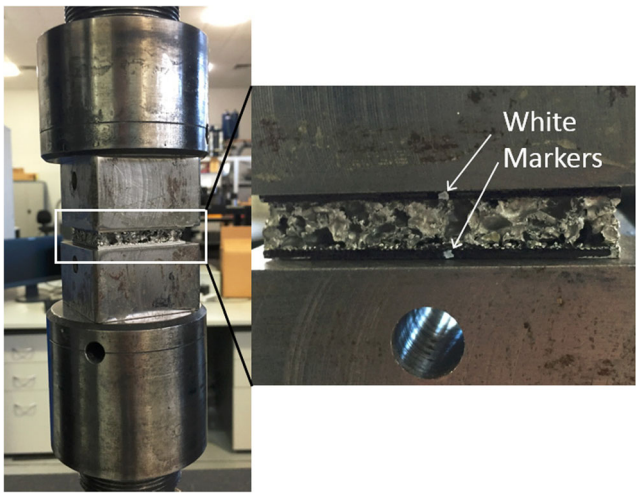

Fig. 4 Compression test [21]. Sample between test plates showing the white markers applied for strain analysis

2.6 V-die bending test

The V-die bending tests were performed using the tooling shown in Fig. 5 in an Instron hydraulic test frame with a 30-kN load cell and a punch profile radius of 15 mm. AFS samples cut in the transverse direction had a length of 100 mm and a width of 20 mm. No lubrication was applied, and the cross-head speed was 0.5 mm/s. Videos were recorded during the test and evaluated visually to enable analysis of material behaviour and failure of the foam material and failure at the interface between the foam and cover sheets. For this, a high-definition camera with a macro objective was used and the picture rate was 1 frame/s. The sample was first aligned with the punch, and the punch moved down until contact was established. After that, the test and the video recording were started. The final part shape after release from the tooling was studied for parts formed to final punch strokes of 5, 6 and 8 mm.

2.7 Roll forming of a V-section

The roll forming trials were performed in a conventional roll forming line (Fig. 6a). A V-section of similar shape compared to that in the V-bending test was formed in four forming passes without lubrication. The "constant length of neutral line" roll forming method was used, where the length of the neutral line in the bend section remains constant throughout all forming passes while the bend radius decreases incrementally [13]. The minimum forming radius in roll forming could be checked visually from the quality of the roll-formed sections after each forming station. The distance between the shaft centres in the roll former was 305 mm, the roll gap set according to the material thickness, and both top and bottom rolls were driven. The forming sequence (flower pattern) is shown in Fig. 6b. AFS strips of 1 m length and 100 mm width were roll formed.

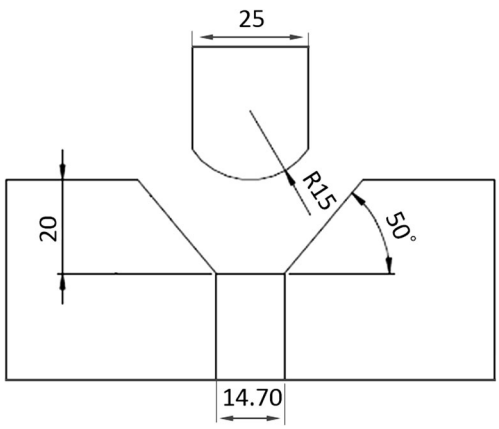

Fig. 5 Schematic of the V-bend test

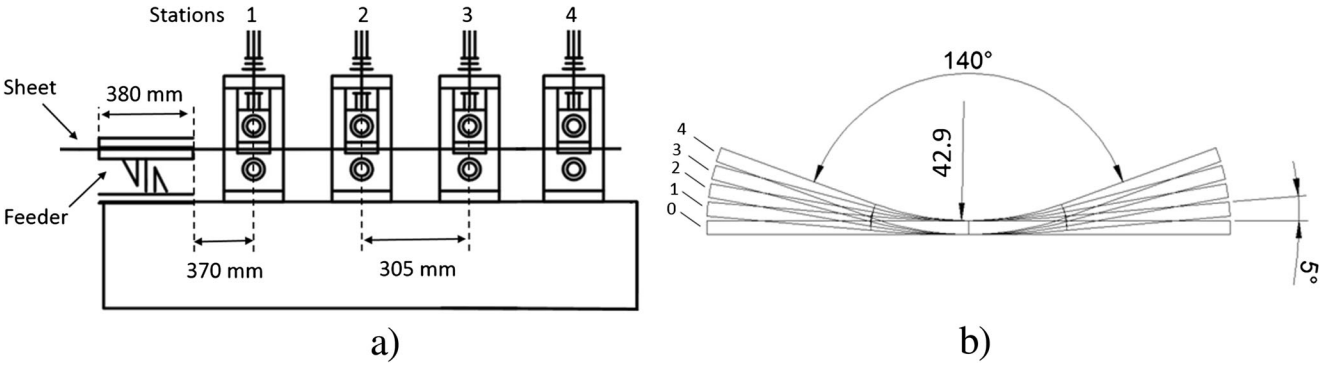

Fig. 6 Roll forming trials: **a** Schematic of the process set up. **b** The forming sequence (flower pattern)

2.8 Analysis of shear deformation in the foam core

The level of shear deformation was estimated by analysing the "gull wing defect". During bending of homogeneous metal strip, the bending legs remain straight. However, in metal laminates where the core layer is weaker than the metal cover sheets, shear deformation of the interlayer generally leads to the curving down of the laminate outside the forming tool [22], as shown schematically in Fig. 8a.

The gull wing defect over the strip width was analysed for the V-bent and the roll-formed sections after forming and release from the forming tool. The samples were sprayed with a white paint and then their top and bottom surfaces scanned using an "ExaScan" 3D scanner. The resolution of the scanned surface was 0.05 mm giving an accuracy of 0.04 mm. 2D section cuts were performed using the software package "Geomagic" [23] at the front and in the centre of the roll-formed components (Fig. 7a) and in the sample centre of the V-bent samples (Fig. 7b).

To measure the gull wing defect, the x and y coordinates of the 2D section cuts were imported into Microsoft Excel and the angle from the x-axis, α, between two accompanying points determined using the relation (Fig. 8b)

$$\alpha = \arctan\left(\frac{\Delta y}{\Delta x}\right) \tag{8}$$

As already mentioned above, in a homogeneous metal sheet without gull wing, the bending legs are straight, leading to a constant value for α outside the profile radius area. In contrast, if there is gull wing, the section legs curve down (Fig. 8a) and α decreases towards the strip edge. In this study, the maximum level of gull wing, $\Delta\alpha$, was defined as

$$\Delta\alpha = \alpha_{\max} - \alpha_{\min} \tag{9}$$

with the maximum and the minimum gull wing angles $\alpha_{\max}$ and $\alpha_{\min}$, respectively (Fig. 8b). Measurements were averaged over the left and the right side of the sample but determined separately for the top and the bottom cover sheets. The maximum level of gull wing was analysed on sections that were roll formed to a final profile radius of 58.4 mm (station

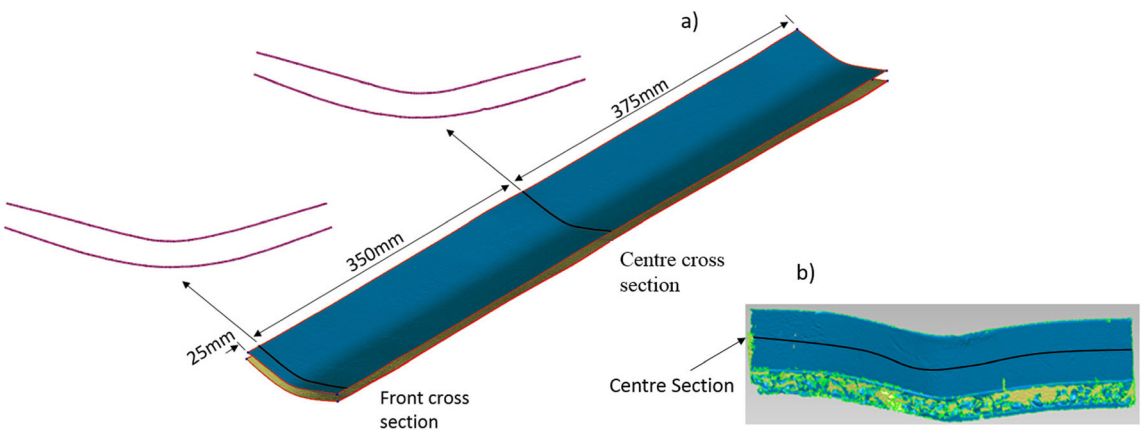

Fig. 7 Scanned part surfaces and 2D section cuts performed in Geomagic: **a** roll-formed profile. **b** V-bent sample section

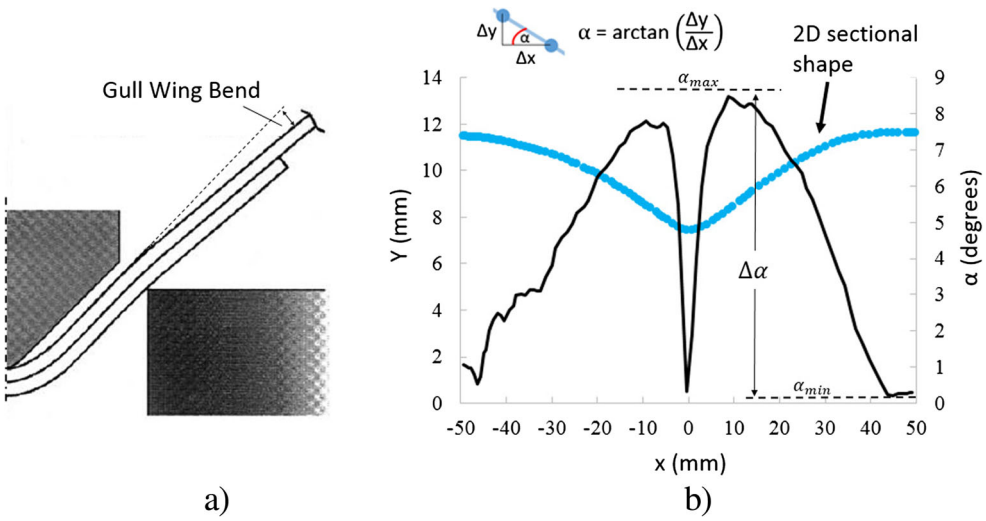

Fig. 8 **a** Schematic of the gull wing bend [24]. **b** 2D sectional shape of the top surface for a sample V-bent to a maximum punch displacement of 5 mm with the distribution of the gull wing angle, α, and the resulting maximum level of gull wing, Δα, shown

3) which represents the minimum profile radius formable without part failure. For V-die bending the gull wing defect was determined for punch strokes of 5, 6 and 8 mm.

2.9 Analysis of material thickness distribution

The thickness of the samples after V-die bending and roll forming was determined using the 3D scan data of the top and bottom surfaces obtained from the ExaScan measurements and 2D section cuts described in Section 2.8 above. Based on the 2D section data, the normal distance from the bottom surface to the top surface was measured, as illustrated in Fig. 9. Material thinning Δt was then determined by subtracting the material thickness, t, measured after forming from the initial laminate thickness of 8.2 mm.

$$\Delta t = 8.2 - t \tag{10}$$

Since material thinning varied depending on the position on the sample, the distribution of thinning along the strip width, x, was examined and plotted.

3 Results and discussion

3.1 Mechanical properties

The tensile tests revealed identical tensile properties for both cover sheets, and therefore, Fig. 10 only shows the true stress–strain curves for cover sheet 1 for the two orientations measured. The mechanical properties are given in Table 1, and only minor planar anisotropy was observed.

The shear stress–strain curves determined in the lab shear tests are shown in Fig. 11. High scatter was observed between the tests, and all samples showed delamination on the

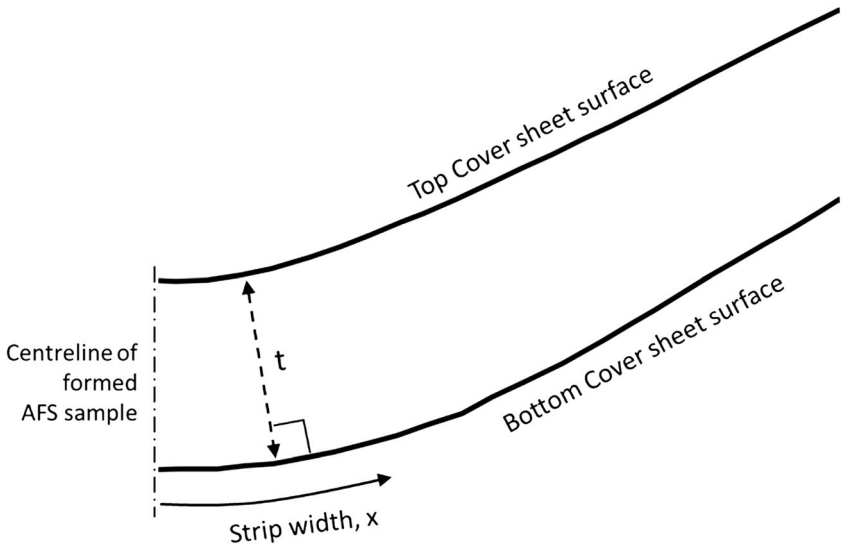

Fig. 9 Schematic of the measurement of thickness, t, over the strip width, x, based on the scanned top and bottom cover sheet surfaces

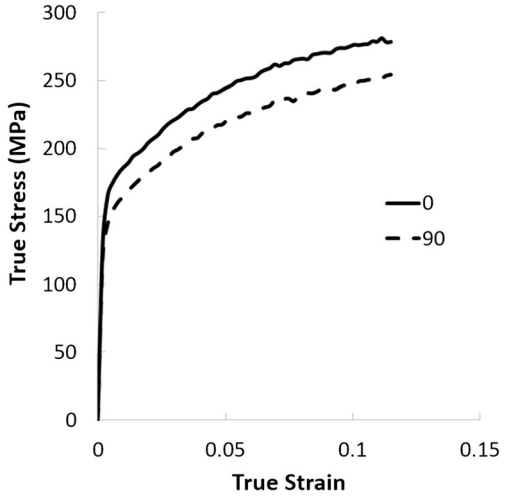

Fig. 10 True stress–strain curves for samples oriented at 0° and 90° to the rolling direction, determined for the AW 5754 cover sheet 1

interface between the core and the cover sheets by failure of the adhesive layer; no residual core layer material was identified on the cover sheets. This suggests that shear deformation mostly occurred in the adhesive between the core and the cover sheet and not in within the aluminium foam core. Under pure shear, deformation failure of the AFS panel can therefore be expected to appear by delamination at the core-cover sheet interface.

The adhesion test revealed a different failure mode compared to the shear test, with fracture mainly situated in the foam interlayer and only minor delamination at the foam core-cover sheet interface (Fig. 12). Significant scatter in the adhesion stress-strain curves can be observed, and this may be due to differences in the failure modes. In samples 1 and 3, failure occurred purely in the foam core. However, for samples 2 and 4, some delamination can be observed at the core-cover sheet interface, which may have resulted in the lower values for maximum adhesion stress observed for those samples. The average maximum adhesion stress is $\sigma_{amax} = 1.68$ MPa± 0.3 MPa (Table 2). A previous study that analysed the tensile properties of ALPORAS® aluminium foam material by conventional tensile tests perpendicular to the core thickness direction reports maximum tensile stress values between 0.8 and 1.44 MPa [25]. The higher level of adhesion stress observed in this study compared to the tensile stress values reported may be related to differences in core density. The same study has shown that the material strength of aluminium foams significantly increases with core density [25]. The high-adhesion strength combined with fracture being majorly situated in the foam interlayer suggests that during tensile loading perpendicular to the AFS material surface, failure is to a large extent governed by the tensile strength of the aluminium foam core.

The compressive stress–strain curves for loading up to a strain of 25% are shown in Fig. 13. The shape of the curves presented here is similar to that reported in previous studies. The average maximum compressive stress is $\sigma_{cmax} = 2.2\ MPa\pm$ 0.07 MPa. Previous studies that analysed the compressive properties of ALPORAS® aluminium foam material by conventional compression tests perpendicular to the core thickness direction report lower values for the maximum compressive stress between 1.46 and 1.84 MPa [25]. Similar to the adhesion test results presented above, the higher values for maximum compressive stress observed in this study may be related to a higher density of the ALPORAS® aluminium foam material tested. At approximately 15% strain, the foam core starts compacting, which can be observed by an increase in the compressive stress. In contrast to previous studies [26], no slippage of the skin layers or extrusion of the core layer at the sample edges was observed.

A summary of the material parameters determined in the laboratory shear, adhesion and compression tests is given in Table 2. It is clear that the values for the Young's Modulus and material strength are very similar between the adhesion and the compression tests, which suggests that material behaviour in both tests was governed by the aluminium foam core. In contrast, the material strength and elastic modulus in shear are significantly lower, which indicates that the material behaviour in the shear test is dominated by the deformation and failure of the adhesive layer between the aluminium foam core and the aluminium cover sheets. This is also confirmed by the failure surfaces shown in Fig. 11. In addition, high scatter can be observed for the adhesion and the lab shear test in regard to τ_{max} and σ_{amax} as well as γ_{max} and ε_{amax}. This indicates that the shear and adhesion properties can vary between different sections of the sandwich panel. This may influence the results when forming large sample dimensions as it is the case in the roll forming trials where 1 m long sections were formed.

Table 1 Mechanical properties of AW 5754 cover sheet 1

Test orientation	Offset yield strength $\sigma_{0.2\%}$ (MPa)	Ultimate tensile strength (MPa)	K	*n*	% uniform elongation
0^0	166	251	436	0.2	11.8
90^0	144	226	540	0.2	12.2

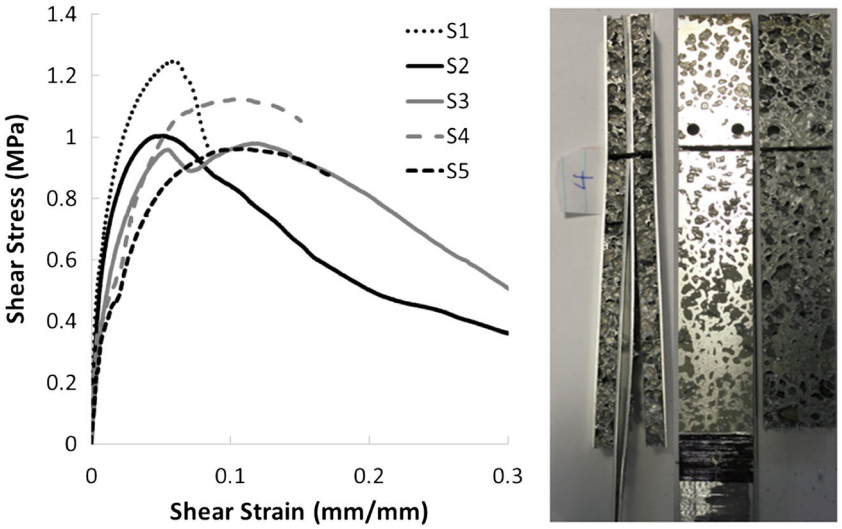

Fig. 11 Shear stress–strain curves determined in the lab shear test and shear test sample 4 showing dominant failure by delamination at the core-cover sheet interface

3.2 V-die bending tests

Figure 14 shows typical load-deflection curves obtained during the V-die bending test. All curves start with an elasto-plastic phase until a peak value is reached, after which the load decreases. Previous studies suggest that the decrease in the punch force is due to compressive deformation of the foam core in the contact zone between the punch and the sheet [12].

However, close inspection of the core layer suggests that the failure mode is a mix of delamination at the core-cover sheet interface and shear fracture of the core (Fig. 14b). It also becomes clear that, in most cases, failure was already initiated at a punch stroke of 3 mm. This indicates that the drop in punch load after 3 mm punch stroke observed (Fig. 14a) may be partly due to the delamination and fracture of the core layer quite early in the test.

3.3 Roll forming trials

Figure 15 shows images of the roll-formed components. Forming of the AFS panels was possible up to the third forming station—corresponding to a minimum radius of ~ 58.4 mm formed at the inner sheet—before initiation of failure in the core was observed.

In some regions of the profile, wrinkles developed at the strip edge. These are due to the delamination of the core layer from the cover sheet, as can be seen in Fig. 15b, and were only observed in some small regions of the profile. Only a small amount of the foam core material remained on the delaminated cover sheet, which suggests that failure occurred in the adhesive layer.

The front and back section views of a roll-formed component are shown in Fig. 16a and b, respectively. At the front, it

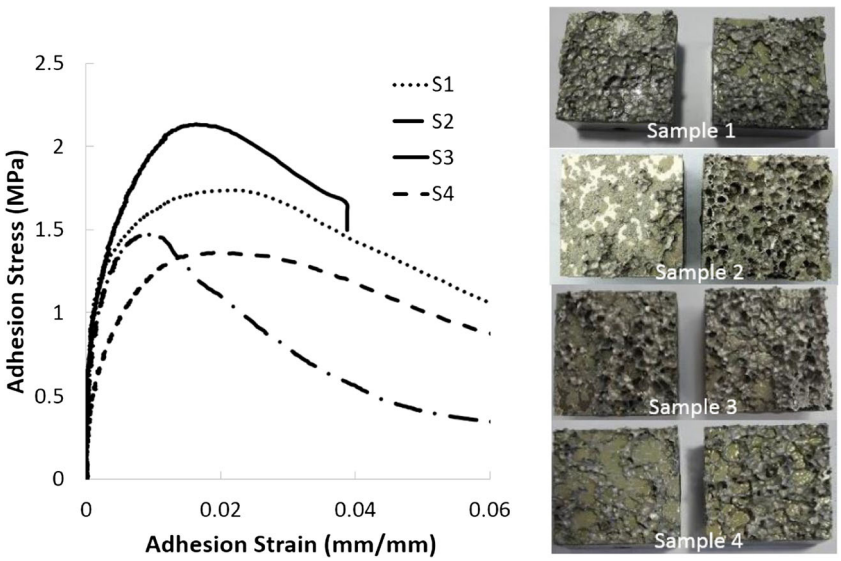

Fig. 12 Adhesion stress–strain curves and failure modes

Table 2 Shear, adhesion and compression properties of the AFS material, providing information about the aluminium foam core and foam core-cover sheet interface

	Lab shear test			Adhesion test			Compression test		
	τ_{max} (MPa)	γ_{max} (%)	G_S (GPa)	σ_{amax} (MPa)	ε_{amax} (%)	E_a (GPa)	σ_{cmax} (MPa)	ε_{cmax} (%)	E_c (GPa)
Average	1.01	8.5	0.12	1.68	2.0	0.93	2.2	3.1	1.0
STDEV	0.13	2.8	0.05	0.3	0.4	0.21	0.07	0.5	0.2

is evident that there is significant compression of the core layer in the centre and the edge regions. The compression in the centre may be due to the contact of the sheet with the upper roll. The compression of the edge could be the result of the sheet being bent over the outer bottom roll radius, which may have led to high-contact pressure and core compression, as can be seen in Fig. 16c. At the back end for some samples, delamination was observed. It is important to note that the front and the back sections of roll-formed components represent the most severe forming conditions, given that at the front, the sheet needs to feed into the next forming station while in the back, the material is not supported by preceding rolls when formed in a particular station [13].

3.4 Comparison of material deformation in roll forming and V-die bending

The final cross-sectional shape after release of the roll-formed section from the roll tooling is compared to that of the V-bent sections formed to final punch strokes of 5 and 8 mm in Fig. 17. Only minor gull wing can be visually observed in the roll-formed section. However, both V-bent strips show significant reverse curvature (gull wing) in the part of the strip that is situated outside the tool, i.e. the region that extends beyond the contact with the bottom die radius. It also can be seen that with increasing punch stroke in V-die bending, there is increased compression of the foam interlayer in the contact zone under the punch. This indicates indentation of the top cover sheet, which is a failure mode that has been observed in previous studies for the bending of AFS panels [12]. In general, Fig. 17 indicates that roll forming enables the forming of a deeper section profile, with less defects, compared to the depth that is possible in V-die bending.

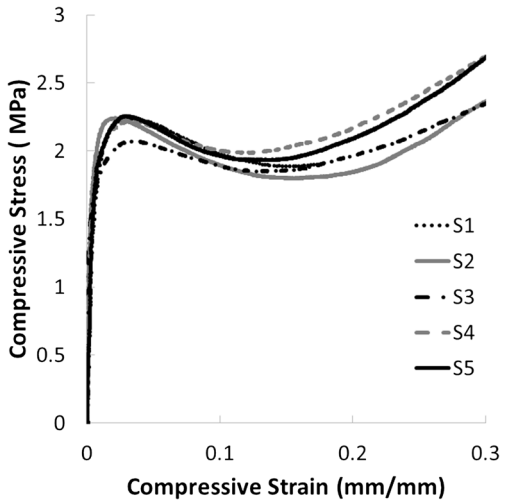

Fig. 13 Compression stress–strain curves

Figure 18 shows the maximum gull wing level, $\Delta\alpha$,measured separately for the top and bottom cover sheets, at the front and centre section of the roll-formed component, and for V-die bending after three levels of punch stroke. The results confirm that there is only very minor gull will in the roll-formed sections which indicates low-shear deformation of the aluminium foam core. Only minor differences in gull wing can be observed when comparing the front and the centre section of the roll-formed strip, which suggests homogeneous forming over the length of the part. In contrast, there is major gull wing in the V-bent sections and the defect increases with increasing punch stroke. Gull wing is also higher in the top compared to the bottom cover sheet. The high gull wing defect is an indication of significant shear deformation in the core layer, and this confirms previous findings that observed shear deformation in V-die bending of AFS panels [27]. The results shown in Fig. 14 suggest that the high-shear deformation and resulting gull wing in the V-bend samples are largely due to shear cracking of the aluminium foam core and delamination of the foam-cover sheet interface. This delamination is an indication of part failure, where the strength and stiffness of these parts would be significantly reduced as a result of this delamination mechanism. Conversely, the small level of gull wing observed in the roll forming trials suggests forming of an intact AFS material without major cracking of the core or delamination issues.

Figure 19 shows the distribution of material thinning over half of the strip width for the V-die bending (for three different punch strokes) and the roll-formed section (front and centre). The thinning measurements shown in Fig. 19 are for the samples where the maximum gull wing measurement, $\Delta\alpha$,is closest to the average value shown in Fig. 18. For all forming conditions, material thinning was observed in the

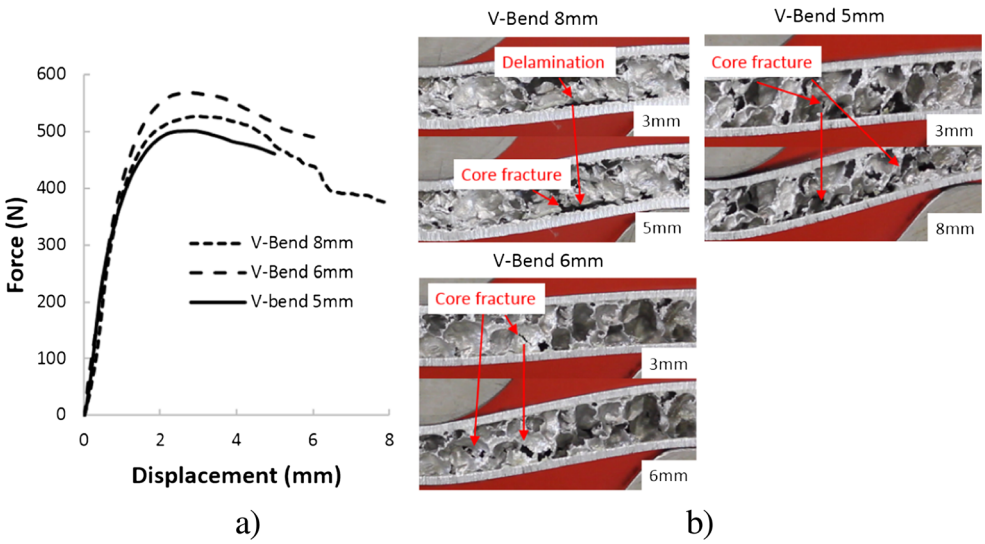

Fig. 14 **a** Representative force displacement curves determined in the V-bending test. **b** Close inspection of core deformation indicating early initiation of core fracture and delamination

punch radius area. The level of thinning was approximately 1 mm for V-die bending to punch strokes of 5 and 6 mm (Fig. 19a) and between 1 and 1.4 mm in the roll-formed sections (Fig. 19b). This suggests that, despite the incremental nature of the roll forming process, there is some crushing of the foam core under the top forming tool. Nevertheless, the profile depths produced when V-die bending to the punch strokes of 5 and 6 mm are significantly lower compared to the profile formed by roll forming (Fig. 17). This may indicate that tool indentation and compression of the aluminium foam core are lower in roll forming compared to V-die bending. The highest reduction in material thickness (approximately 2.0 mm) was determined for the V-die bending to a final punch stroke of 8 mm (Fig. 19a) which may explain the high level of gull wing observed for this forming condition. In addition to a reduced material thickness in the profile radius, the roll-formed section also shows some material thinning in the outer strip edge (Fig. 19b). This thinning has already been visually observed in section 3.3 and related to a high-contact stress between the strip and the bottom roll (see Fig. 16c).

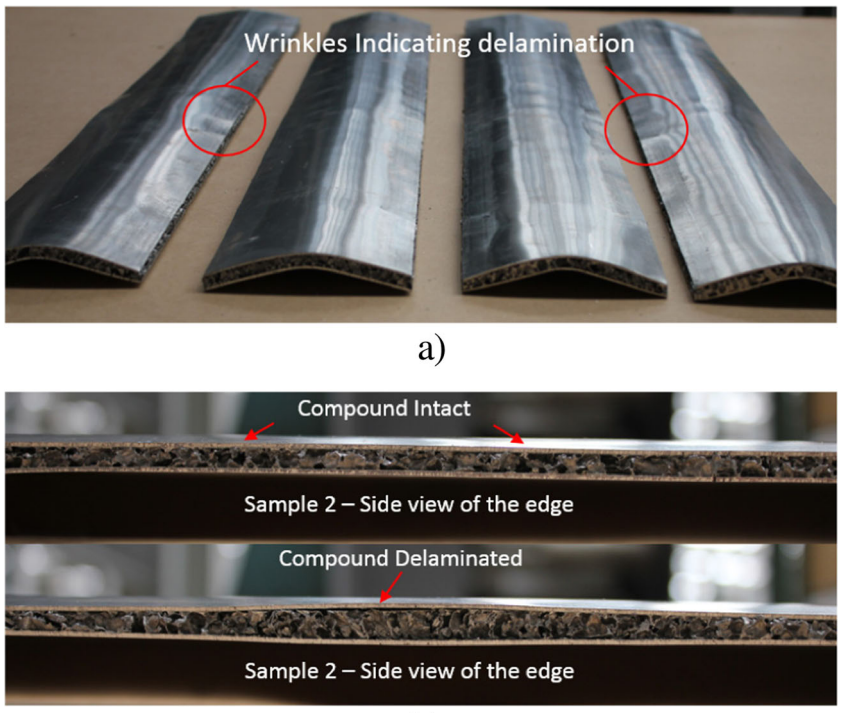

Fig. 15 Roll-formed parts. **a** Wrinkles indicating some delaminated areas. **b** View of the strip edge of an intact section length and a delaminated section length

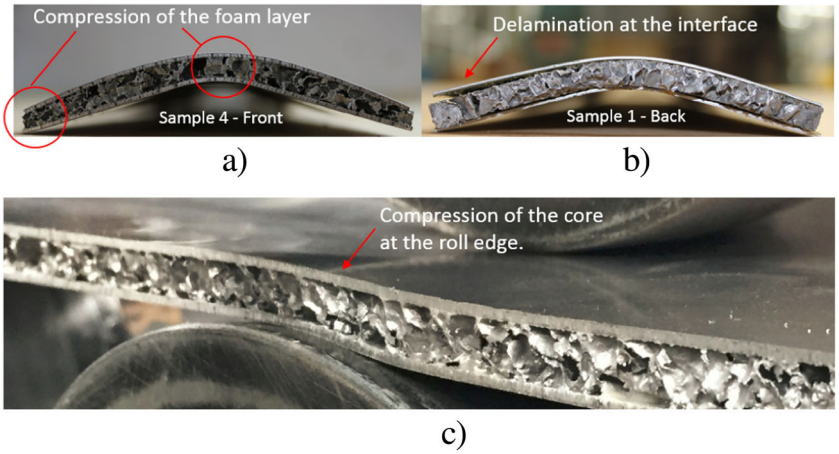

Fig. 16 Roll-formed components. **a** Front section showing compression in the profile radius and the edge. **b** Back section showing delamination. **c** Strip edge bent over the outer roll radius indicating compression of the core

4 Discussion

The V-die bending tests revealed early failure of the laminate by shear fracture and delamination at the foam-cover sheet interface. It is well known that the bending of laminates that consist of strong cover sheets bonded to a relatively weak core material leads to high-shear deformation of the core [8]. Previous work suggested that, for the successful forming of AFS materials, adhesion and shear strength of the core layer need to be as high as possible [10]. The laminate investigated in this study was ex-situ bonded with an adhesive, and previous work has revealed that this type of laminate is much more prone to early failure by delamination at the core-cover sheet interface compared to metallurgical bonded counterparts [12]. This is verified by the shear tests of this study, which identified very low shear adhesion strength and early failure by delamination in the adhesive layer in the V-die bending trials. This indicates that the low formability observed in the V-die bending tests of this study is primarily due to the low-shear adhesion strength of the laminate at the core-cover sheet interface.

Despite this, the material was successfully roll formed to a V-section profile of significant depth without major failure. The roll-formed sections also showed significantly less gull wing defect compared with the V-bent counterparts, and this indicates that shear deformation and delamination of the interlayer were minor. One reason for this may be the incremental nature of the process where the material is formed in successive roll stands [28]. This could have led to a more evenly distributed contact on the upper cover sheet compared with V-die bending and therefore lower indentation and compressive deformation of the foam core and reduced shear stresses in the interlayer. The indentation of the top cover sheet by the V-die bending punch was observed in V-die bending at high-punch displacement but was found to be small in the roll-formed sections (see Fig. 17, 19a and b). Previous studies have revealed that the full tool contact provided by the top and bottom rolls in roll forming leads to more homogeneous material deformation and hence less shape defects compared to V-die bending [16].

Some shape defects were observed in the roll forming trials, such as the compression of the foam layer at the strip edge which is related to high-contact pressures between the bottom roll and the strip edge (Fig. 16c). In addition, some localised areas showed delamination in the strip edge over the length of the part and the development of wrinkles. In roll forming, the

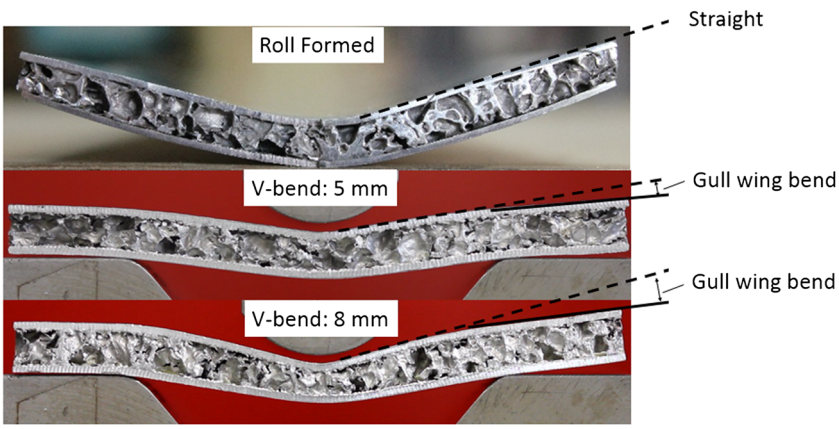

Fig. 17 Comparison of final shape after roll forming and V-bending to 5 and 8 mm punch displacement with gull wing defect in bent samples schematically indicated

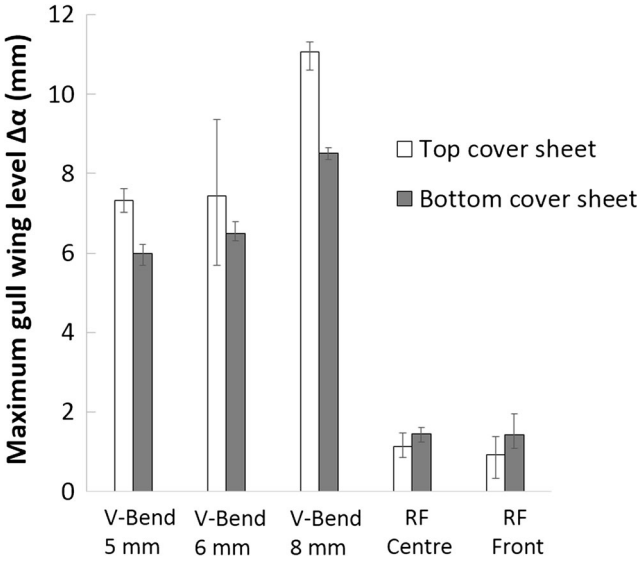

Fig. 18 Maximum level of gull wing determined in the V-bend tests at maximum punch stroke of 5, 6 and 8 mm and on section cuts taken in the front and the centre of the roll formed (RF) components

strip edge travels a longer distance compared to the centre-line section and this leads to longitudinal deformation in the strip edge. If this deformation is in the plastic range, compressive stresses in the longitudinal direction and wrinkling of the strip edge can result when the material leaves the roll station [13]. This defect can be controlled with an improved bending sequence or flower design.

Another explanation of the delamination observed at the strip edge could be the bending and re-straightening deformation over the bottom roll that is generally required when the material enters the roll gap [29]. Previous studies performed on the channel drawing of metal laminates have revealed that such deformation can lead to shear in combination with transverse stresses perpendicular to the core-cover sheet interface and through that to delamination [30]. The shear adhesion strength of the ex-situ bonded laminate used in this study was low (Fig. 11) while the adhesion strength showed high variation between samples (Fig. 12). These factors, in combination with the observation that delamination at the strip edge was only observed in distinct areas over the strip length of the roll-formed components, suggest that this shape defect is possibly due to a low and inhomogeneous adhesion strength between the core and the cover sheet material. Therefore, improved part quality could be achieved by roll forming metallurgical bonded AFS materials that generally show higher adhesion strength. In addition, the severity of forming the material over the bottom roll radius can be reduced by increasing the roll diameter [29].

5 Conclusion

A commercial and ex-situ bonded aluminium foam sandwich (AFS) material was formed to a simple V-section profile by V-die bending and roll forming.

Tensile-adhesion, compression and lap shear tests were performed and revealed that the behaviour of the AFS material in tension and compression is governed by the aluminium foam core, while the shear strength was low due to failure of the adhesive layer at the core-cover sheet interface.

In V-die bending, early delamination of the AFS material was observed and related to high-shear deformation of the core layer as a result of the core-cover sheet strength mismatch. In addition, shear fracture of the core was observed.

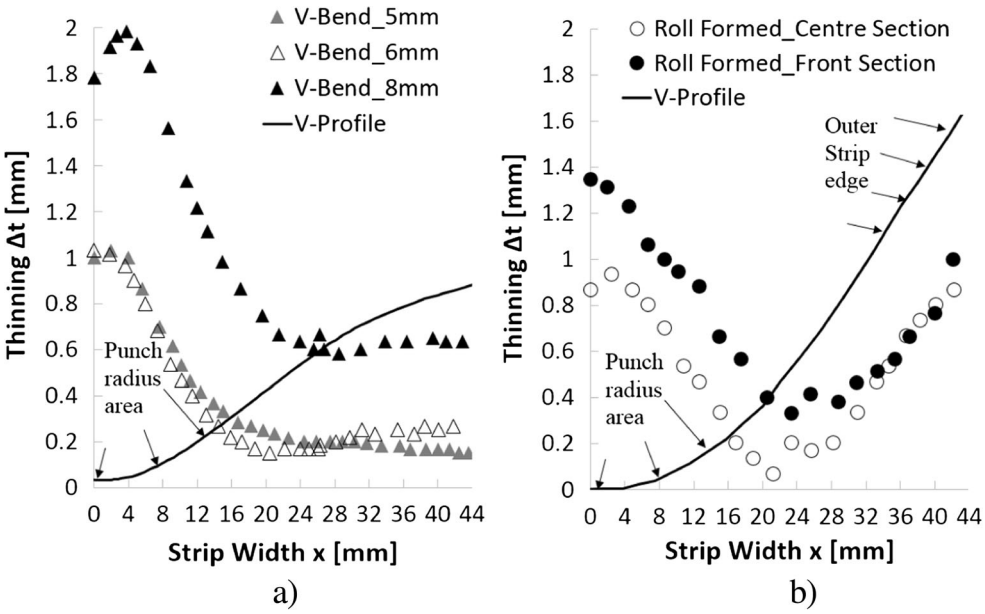

Fig. 19 Distribution of material thickness over half the strip width for the following: **a** V-bend tests at maximum punch stroke of 5, 6 and 8 mm. **b** Roll forming centre and front section

The early failure of the AFS material in shear manifests itself by a high-gull wing defect in the V-die bent samples.

In roll forming, only minor gull wing defect was observed for the forming of a similar part shape, indicating low-shear deformation and an intact adhesion at the core-cover sheet interface. Some delamination in the strip edge was observed. This was related to the bending and re-straightening of the material when entering the roll gap in combination with the low-adhesion strength at the core-cover sheet interface. This issue may be resolved by an improved roll design and by forming metallurgical bonded AFS sheets with higher core-cover sheet adhesion strength.

In general, the results of this study suggest that roll forming represents a promising alternative to conventional stamping or bending for the forming of AFS components. Shear deformation in roll forming was lower in comparison to V-die bending, and this led to reduced shape defects and the successful forming of longitudinal components that are of interest to the transport, solar and housing industries.

Even though the current study is limited to AFS panels, the findings of this work are applicable to the forming of other metal hybrid materials (for example metal/carbon fibre laminates), which are receiving increasing attention for weight reduction in the transport industry.

Acknowledgements The authors would like to acknowledge the assistance of Emeritus Professor J.L. Duncan in writing this paper. The authors further would like to thank Josu Azkune, John Hore and Marius Kaiser for their assistance in the experimental work of this paper.

Funding information The authors further appreciate the financial support of the Australian Research Council (ARC Linkage grant—LP120100111), the Wuhan Iron and Steel (Group) Corp (WISCO), DataM Sheet Metal Solutions and Australian Rollforming Manufacturers and the Global Training 2012 Program of the Basque Government.

References

1. Banhart J, Seeliger HW (2008) Aluminium foam sandwich panels: manufacture, metallurgy and applications. Adv Eng Mater 10(9): 793–802
2. Banhart J, Seeliger H-W (2012) Recent trends in aluminum foam sandwich technology. Adv Eng Mater 14(12):1082–1087
3. Schwingel D, Seeliger H-W, Vecchionacci C, Alwes D, Dittrich J (2007) Aluminium foam sandwich structures for space applications. Acta Astronaut 61(1–6):326–330
4. Nassar H, Albakri M, Pan H, Khraisheh M (2012) On the gas pressure forming of aluminium foam sandwich panels: experiments and numerical simulations. CIRP Ann Manuf Technol 61(1):243–246
5. Contorno D, Filice L, Fratini L, Micari F (2006) Forming of aluminum foam sandwich panels: numerical simulations and experimental tests. J Mater Process Technol 177(1–3):364–367
6. Jackson KP, Allwood JM, Landert M (2008) Incremental forming of sandwich panels. J Mater Process Technol 204(1–3):290–303
7. Wang J, Yang C-K (2013) Failure analysis of hydroforming of sandwich panels. J Manuf Process 15(2):256–262
8. Weiss M, Rolfe BF, Dingle M, Duncan JL (2005) Elastic bending of steel-polymer-steel (SPS) laminates to a constant curvature. J Appl Mech 73(4):574–579
9. Zu G, Song B, Zhong Z, Li X, Mu Y, Yao G (2012) Static three-point bending behavior of aluminum foam sandwich. J Alloys Compd 540:275–278
10. Mohr D (2005) On the role of shear strength in sandwich sheet forming. Int J Solids Struct 42(5–6):1491–1512
11. Zu G-y, Lu R-h, Li X-b, Zhong Z-y, Ma X-j, Han M-b, Yao G-c (2013) Three-point bending behavior of aluminum foam sandwich with steel panel. Trans Nonferrous Metals Soc China 23(9):2491–2495
12. Crupi V, Montanini R (2007) Aluminium foam sandwiches collapse modes under static and dynamic three-point bending. Int J Impact Eng 34(3):509–521
13. Halmos GT (2005) Roll forming handbook, CRC Press, Taylor & Francis Group, ISBN: 0824795636
14. Badr OM, Rolfe B, Hodgson P, Weiss M (2015) Forming of high strength titanium sheet at room temperature. Mater Des , Part B 66: 618–626
15. Abeyrathna B, Rolfe B, Weiss M (2017) The effect of process and geometric parameters on longitudinal edge strain and product defects in cold roll forming. Int J Adv Manuf Technol:1–12
16. Marnette J, Weiss M, Hodgson PD (2014) Roll-formability of cryo-rolled ultrafine aluminium sheet. Mater Des 63:471–478
17. AS1391—1991 (1991) "Methods for tensile testing of metals"
18. ASTM-D3528 "Standard Test Method for Strength Properties of Double Lap Shear Adhesive Joints by Tension Loading", 2008
19. ASTM-C273 "Standard Test Method for Shear Properties of Sandwich Core Materials", (2011) 7
20. ASTM-C297 "Standard Test Method for Flatwise Tensile Strength of Sandwich Constructions", (2010)
21. ASTM-C365 "Standard Test Method for Flatwise Compressive Properties of Sandwich Cores", (2011)
22. Weiss M, Dingle ME, Rolfe BF, Hodgson PD (2007) The influence of temperature on the forming behavior of metal/polymer laminates in sheet metal forming. J Eng Mater Technol Trans ASME 129(4): 530–537
23. Geomagic Qualify (2014) Available: http://www.geomagic.com/en/
24. Takiguchi M, Yoshida F (2003) Analysis of plastic bending of adhesive-bonded sheet metals taking account of viscoplasticity of adhesive. J Mater Process Technol 140(1–3):441–446
25. Andrews E, Sanders W, Gibson LJ (1999) Compressive and tensile behaviour of aluminum foams. Mater Sci Eng A 270(2):113–124
26. Casavola C, Dell'Orco V, Giannoccaro R, Pappalettere C (2009) Structural response of Aluminium foam sandwich under compressive loading. SEM Annual Conference, Albuquerque New Mexico USA
27. Zhenzhong S, Weifeng H, Haibin C, Shenggui C, Rongyong L (2011) Study on V-bending of Aluminium foam sandwich panels, Adv Mater Res Vols 181-182:281–286
28. Badr OM, Rolfe B, Hodgson P, Weiss M (2013) Experimental study into the correlation between the incremental forming and the nature of springback in automotive steels. Int J Mater Prod Technol 47(1–4):150–161
29. Abeyrathna B, Rolfe B, Hodgson P, Weiss M (2017) Local deformation in roll forming. Int J Adv Manuf Tech 88(9–12):2405–2415
30. Kim JK, Thomson PF (1990) Separation behaviour of sheet steel laminate during forming. J Mater Process Technol 22(2):147–161